Neutral-Current and Day-Night Measurements from the Pure D_2O Phase in SNO

R. Tafirout
Laurentian University, Sudbury, Ontario, Canada

For the SNO Collaboration

August 22, 2003

Abstract

Observations of ν interactions on deuterium and measurements of day and night solar neutrino energy spectra and rates in the Sudbury Neutrino Observatory are reported. Assuming the standard ^{8}B shape, the measured ν_e component of the ^{8}B flux (ϕ_e), and the non-ν_e component ($\phi_{\mu\tau}$) provide strong evidence for ν_e flavor transformation. The total flux measured with the neutral current reaction is consistent with solar models. A global solar neutrino MSW analysis strongly favors the LMA solution.

1 Introduction

The Sudbury Neutrino Observatory (SNO) [1] is a water Cherenkov detector located at a depth of 6010 m of water equivalent in the INCO, Ltd. Creighton mine near Sudbury, Ontario, Canada. The detector uses ultra-pure heavy water contained in a transparent acrylic spherical shell 12 m in diameter to detect solar neutrinos. Cherenkov photons generated in the heavy water are detected by 9456 photomultiplier tubes (PMTs) mounted on a stainless steel geodesic sphere 17.8 m in diameter. The geodesic sphere is immersed in ultra-pure light water to provide shielding from radioactivity in both the PMT array and the cavity rock. SNO detects ^{8}B solar neutrinos through the

reactions:

$$\begin{array}{lcll} \nu_e + \mathrm{d} & \rightarrow & \mathrm{p} + \mathrm{p} + \mathrm{e}^- & \text{(CC)}, \\ \nu_x + \mathrm{d} & \rightarrow & \mathrm{p} + \mathrm{n} + \nu_x & \text{(NC)}, \\ \nu_x + \mathrm{e}^- & \rightarrow & \nu_x + e^- & \text{(ES)}. \end{array}$$

The charged current reaction (CC) is sensitive exclusively to electron-type neutrinos, while the neutral current reaction (NC) is equally sensitive to all active neutrino flavors ($x = e, \mu, \tau$). The elastic scattering reaction (ES) is sensitive to all flavors as well, but with reduced sensitivity to ν_μ and ν_τ. Sensitivity to these three reactions allows SNO to determine the electron and non-electron active neutrino components of the solar flux. We present here the first NC and day-night results from SNO [2, 3].

2 Data

The data reported here were recorded between Nov. 2, 1999 and May 28, 2001 and represent a total of 306.4 live days, spanning the entire first phase of the experiment, in which only D_2O was present in the sensitive volume. PMT times and hit patterns were used to reconstruct event vertices and directions and to assign to each event a most probable kinetic energy, T_{eff}. The total flux of active ^{8}B solar neutrinos with energies greater than 2.2 MeV (the NC reaction threshold) was measured with the NC signal (Cherenkov photons resulting from the 6.25 MeV γ ray from neutron capture on deuterium). The analysis threshold was $T_{\text{eff}} \geq 5$ MeV. Above this energy threshold, there were contributions from CC events in the D_2O, ES events in the D_2O and H_2O, capture of neutrons (both from the NC reaction and backgrounds), and low energy Cherenkov background events. Only events which had reconstructed vertices within 550 cm from the detector center were accepted, yielding 2928 events in the energy region selected for analysis, 5 to 20 MeV.

3 Backgrounds

The primary backgrounds to the NC signal are due to low levels of uranium and thorium decay chain daughters (^{214}Bi and ^{208}Tl) in the detector materials. These activities generate free neutrons in the D_2O, from deuteron photodisintegration (pd), and low energy Cherenkov events. *Ex-situ* assays and *in-situ* analysis of the low energy ($4 - 4.5$ MeV) Cherenkov signal region

provide independent uranium and thorium photodisintegration background measurements. The total photodisintegration background corresponds to approximately 12% of the number of NC neutrons predicted by the standard solar model from ^{8}B neutrinos.

Table 1 shows the number of photodisintegration and Cherenkov background events (including systematic uncertainties) due to activity in the D_2O (internal region), acrylic vessel (AV), H_2O (external region), and PMT array. Other sources of free neutrons in the D_2O region are cosmic ray events and atmospheric neutrinos. To reduce these backgrounds, an additional neutron background cut imposed a 250-ms deadtime (in software) following every event in which the total number of PMTs which registered a hit was greater than 60.

4 Neutrino fluxes

In order to test the null hypothesis, the assumption that there are only electron neutrinos in the solar neutrino flux, the data, as shown in Figure 1, are resolved into contributions from CC, ES, and NC events above threshold using pdfs in $T_{\rm eff}$, $\cos\theta_\odot$, and $(R/R_{\rm AV})^3$, derived from Monte Carlo calculations generated assuming no flavor transformation and the standard ^{8}B spectral shape. Background event pdfs are included in the analysis with fixed amplitudes determined by the background calibration. The extended maximum likelihood method used in the signal decomposition yields $1967.7^{+61.9}_{-60.9}$ CC events, $263.6^{+26.4}_{-25.6}$ ES events, and $576.5^{+49.5}_{-48.9}$ NC events, where only statistical uncertainties are given. Systematic uncertainties on fluxes are obtained by repeating the signal decomposition with perturbed pdfs (constrained by calibration data).

Normalized to the integrated rates above the kinetic energy threshold of $T_{\rm eff} \geq 5$ MeV, the flux of ^{8}B neutrinos measured with each reaction is (in units of 10^6 cm^{-2}s^{-1}):

$$\begin{aligned}
\phi_{\rm CC}^{\rm SNO} &= 1.76^{+0.06}_{-0.05}({\rm stat.})^{+0.09}_{-0.09}\ ({\rm syst.}) \\
\phi_{\rm ES}^{\rm SNO} &= 2.39^{+0.24}_{-0.23}({\rm stat.})^{+0.12}_{-0.12}\ ({\rm syst.}) \\
\phi_{\rm NC}^{\rm SNO} &= 5.09^{+0.44}_{-0.43}({\rm stat.})^{+0.46}_{-0.43}\ ({\rm syst.}).
\end{aligned}$$

The excess of the NC flux over the CC and ES fluxes implies neutrino flavor transformations. A simple change of variables resolves the data directly into

electron (ϕ_e) and non-electron ($\phi_{\mu\tau}$) components,

$$\begin{aligned} \phi_e &= 1.76^{+0.05}_{-0.05}(\text{stat.})^{+0.09}_{-0.09}\ (\text{syst.}) \\ \phi_{\mu\tau} &= 3.41^{+0.45}_{-0.45}(\text{stat.})^{+0.48}_{-0.45}\ (\text{syst.}) \end{aligned}$$

Combining the statistical and systematic uncertainties in quadrature, $\phi_{\mu\tau}$ is $3.41^{+0.66}_{-0.64}$, which is 5.3σ above zero, providing strong evidence for flavor transformation consistent with neutrino oscillations. Figure 2 shows the flux of non-electron flavor active neutrinos vs the flux of electron neutrinos deduced from the SNO data.

5 Day-Night

The flavor conversion can be explained by neutrino oscillation models based on flavor mixing. For some values of the mixing parameters, spectral distortions and a measurable dependence on solar zenith angle are expected. The latter might be caused by interaction with the matter of the Earth (the MSW effect) and would depend not only on oscillation parameters and neutrino energy, but also on the path length and e^- density through the Earth.

The measured night and day fluxes ϕ_N and ϕ_D were used to form the asymmetry ratio for each reaction: $\mathcal{A} = 2(\phi_N - \phi_D)/(\phi_N + \phi_D)$. Active-only neutrino models predict $\mathcal{A}_{NC} = 0$. The same models allow $\mathcal{A}_{CC} \neq 0$.

Table 2 (a) shows the results for $\mathcal{A}_e$ derived from the CC day and night rate measurements, i.e., $\mathcal{A}_e = \mathcal{A}_{CC}$. The day and night flavor contents were then extracted by changing variables to $\phi_{CC} = \phi_e$, $\phi_{NC} = \phi_{tot} = \phi_e + \phi_{\mu\tau}$ and $\phi_{ES} = \phi_e + \epsilon\phi_{\mu\tau}$, where $\epsilon \equiv 1/6.48$ is the ratio of the average ES cross sections above 5 MeV for $\nu_{\mu\tau}$ and ν_e. Table 2 (b) shows the asymmetries of ϕ_e and ϕ_{tot} with this additional constraint from the ES rate measurements. This analysis allowed for an asymmetry in the total flux of ^{8}B neutrinos (non-zero $\mathcal{A}_{tot}$), with the measurements of $\mathcal{A}_e$ and $\mathcal{A}_{tot}$ having a strong anti-correlation. Figure 3 shows the $\mathcal{A}_e$ vs. $\mathcal{A}_{tot}$ joint probability contours. Forcing $\mathcal{A}_{tot} = 0$, as predicted by active-only models, yielded the result in Table 2 (c) of $\mathcal{A}_e = 7.0\% \pm 4.9\%\ (\text{stat.})^{+1.3}_{-1.2}\%\ (\text{sys.})$. The Super-Kamiokande (SK) collaboration measured $\mathcal{A}_{ES}(SK) = 3.3\% \pm 2.2\%\ (\text{stat.})^{+1.3}_{-1.2}\%\ (\text{sys.})$. The ES measurement includes a neutral current component, which reduces the asymmetry for this reaction relative to $\mathcal{A}_e$. $\mathcal{A}_{ES}(SK)$ may be converted to an equivalent electron flavor asymmetry using the total neutrino flux measured by SNO, yielding

$\mathcal{A}_e(SK)$ (Table 2 (d)). This value is in good agreement with SNO's direct measurement of $\mathcal{A}_e$, as seen in Figure 3.

SNO's day and night energy spectra (Figure 4) have also been used to produce MSW exclusion plots and limits on neutrino flavor mixing parameters. MSW oscillation models between two active flavors were fit to the data. There are 3 free parameters in the fit: the total ^{8}B flux ϕ_B, the difference Δm^2 between the squared masses of the two neutrino mass eigenstates, and the mixing angle θ. Figure 5(a) shows allowed mixing parameter regions using only SNO data with no additional experimental constraints or inputs from solar models. By including flux information from the Cl and Ga experiments, the day and night spectra from the SK experiment, along with solar model predictions for the more robust *pp*, *pep* and ^{7}Be neutrino fluxes, the contours shown in Figure 5(b) were produced. This global analysis strongly favors the Large Mixing Angle (LMA) region (see Table 3), and $\tan^2\theta < 1$.

6 Summary

The results presented here are the first direct measurement of the total flux of active ^{8}B neutrinos arriving from the sun and provide strong evidence for neutrino flavor transformation. The total flux of ^{8}B neutrinos measured with the NC reaction is in agreement with the SSM prediction. A global fit to SNO's day and night energy spectra and data from other solar neutrino experiments strongly favors the LMA solution in a 2-flavor MSW neutrino oscillation analysis.

This research was supported by: Canada: NSERC, Industry Canada, NRC, Northern Ontario Heritage Fund Corporation, Inco, AECL, Ontario Power Generation; US: Dept. of Energy; UK: PPARC. We thank the SNO technical staff for their strong contributions.

References

[1] The SNO collaboration, Nucl. Instr. and Meth. **A449**, 172 (2000).

[2] Q.R. Ahmad *et al.*, Phys. Rev. Lett. **89**, 011301 (2002);

[3] Q.R. Ahmad *et al.*, Phys. Rev. Lett. **89**, 011302 (2002);

Table 1: Neutron and Cherenkov background events.

Source	Events
D_2O photodisintegration	44^{+8}_{-9}
H_2O + AV photodisintegration	27^{+8}_{-8}
Atmospheric ν's and sub-Cherenkov threshold μ's	4 ± 1
Fission	$\ll 1$
$^2H(\alpha, \alpha)pn$	2 ± 0.4
$^{17}O(\alpha,n)$	$\ll 1$
Terrestrial and reactor $\bar{\nu}$'s	1^{+3}_{-1}
External neutrons	$\ll 1$
Total neutron background	78 ± 12
D_2O Cherenkov	20^{+13}_{-6}
H_2O Cherenkov	3^{+4}_{-3}
AV Cherenkov	6^{+3}_{-6}
PMT Cherenkov	16^{+11}_{-8}
Total Cherenkov background	45^{+18}_{-12}

Table 2: Measurement of the ϕ_e and ϕ_{tot} asymmetry for various constraints. All analyses assume an undistorted ^{8}B spectrum.

Constraints	Asymmetry (%)
a) no additional constraint	$\mathcal{A}_{CC} = 14.0 \pm 6.3^{+1.5}_{-1.4}$ $\mathcal{A}_{NC} = -20.4 \pm 16.9^{+2.4}_{-2.5}$
b) $\phi_{ES} = (1-\epsilon)\phi_e + \epsilon\phi_{tot}$	$\mathcal{A}_e = 12.8 \pm 6.2^{+1.5}_{-1.4}$ $\mathcal{A}_{tot} = -24.2 \pm 16.1^{+2.4}_{-2.5}$
c) $\phi_{ES} = (1-\epsilon)\phi_e + \epsilon\phi_{tot}$ $\mathcal{A}_{tot} = 0$	$\mathcal{A}_e = 7.0 \pm 4.9^{+1.3}_{-1.2}$
d) $\phi_{ES} = (1-\epsilon)\phi_e + \epsilon\phi_{tot}$ $\mathcal{A}_{tot} = 0$ $\mathcal{A}_{ES}(SK) = 3.3\% \pm 2.2\%^{+1.3\%}_{-1.2\%}$	$\mathcal{A}_e(SK) = 5.3 \pm 3.7^{+2.0}_{-1.7}$ (derived from SK $\mathcal{A}_{ES}$ and SNO total ^{8}B flux)

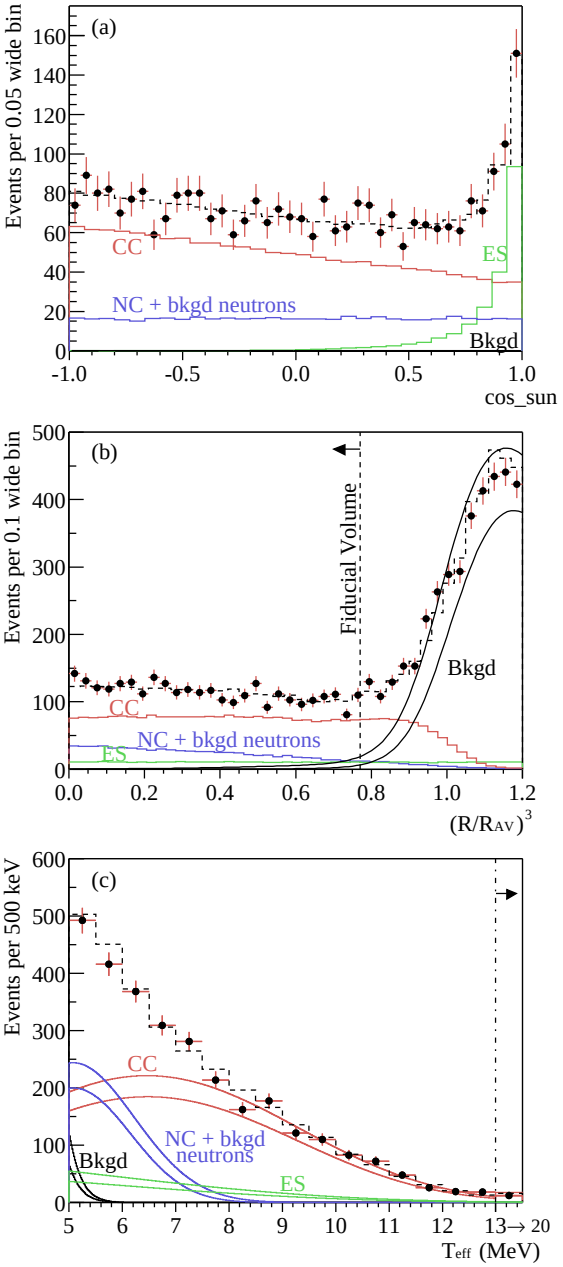

Figure 1: (a) Distribution of $\cos\theta_\odot$ for $R \leq 550$ cm. (b) Distribution of the volume weighted radial variable $(R/R_{\rm AV})^3$. (c) Kinetic energy for $R \leq 550$ cm. Also shown are the Monte Carlo predictions for CC, ES and NC + bkgd neutron events scaled to the fit results, and the calculated spectrum of Cherenkov background (Bkgd) events. The dashed lines represent the summed components, and the bands show $\pm 1\sigma$ uncertainties.

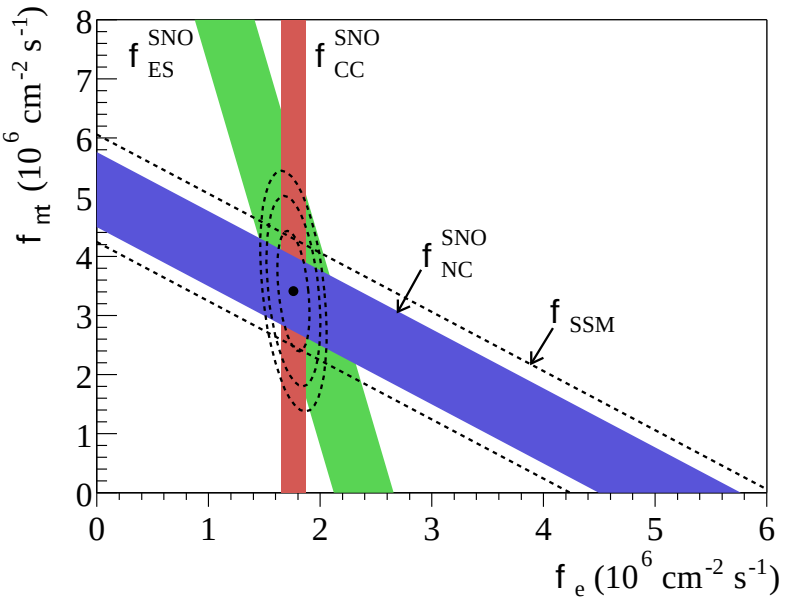

Figure 2: Flux of ^{8}B solar neutrinos which are μ or τ flavor vs flux of electron neutrinos deduced from the three neutrino reactions in SNO. The diagonal bands show the total ^{8}B flux as predicted by the SSM [**?**] (dashed lines) and that measured with the NC reaction in SNO (solid band). The intercepts of these bands with the axes represent the $\pm 1\sigma$ errors. The bands intersect at the fit values for ϕ_e and $\phi_{\mu\tau}$, indicating that the combined flux results are consistent with neutrino flavor transformation assuming no distortion in the ^{8}B neutrino energy spectrum. The error ellipses represent the 68%, 95%, and 99% joint probability contours for ϕ_e and $\phi_{\mu\tau}$.

Table 3: Best fit points in the MSW plane for global MSW analysis using all solar neutrino data. ϕ_B is the best-fit ^{8}B flux for each point, and has units of 10^6 cm^{-2} s^{-1}. Δm^2 has units of eV^2. $\mathcal{A}_e$ is the predicted asymmetry for each point.

Region	χ^2_{min}/dof	ϕ_B	$\mathcal{A}_e$(%)	Δm^2	$\tan^2\theta$	c.l.(%)
LMA	57.0/72	5.86	6.4	5.0×10^{-5}	0.34	—
LOW	67.7/72	4.95	5.9	1.3×10^{-7}	0.55	99.5

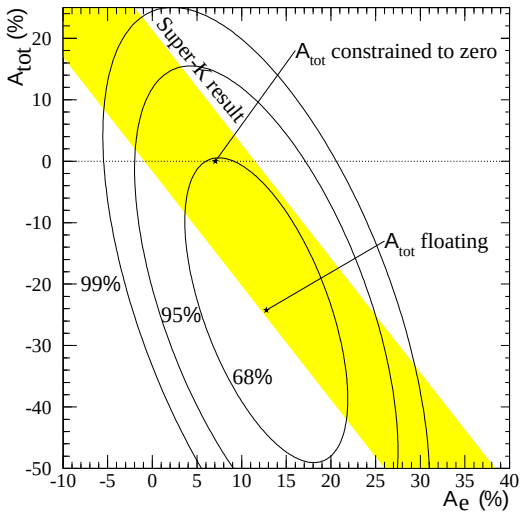

Figure 3: Joint probability contours for $\mathcal{A}_{tot}$ and $\mathcal{A}_e$. The points indicate the results when $\mathcal{A}_{tot}$ is allowed to float and when it is constrained to zero. The diagonal band indicates the 68% joint contour for the Super-K $\mathcal{A}_{ES}$ measurement.

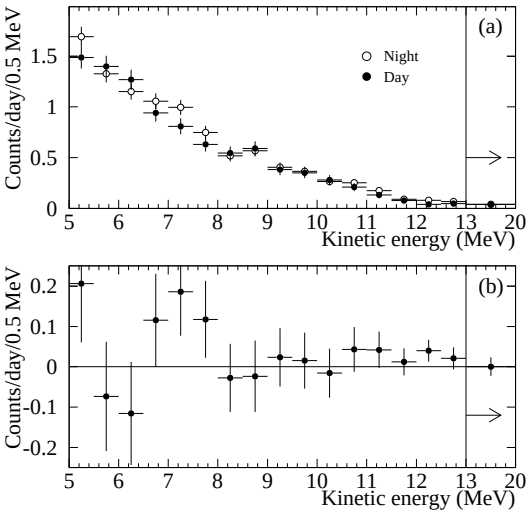

Figure 4: (a) Energy spectra for day and night. All signals and backgrounds contribute. The final bin extends from 13.0 to 20.0 MeV. (b) Difference, *night - day*, between the spectra. The day rate was 9.23 ± 0.27 events/day, and the night rate was 9.79 ± 0.24 events/day.

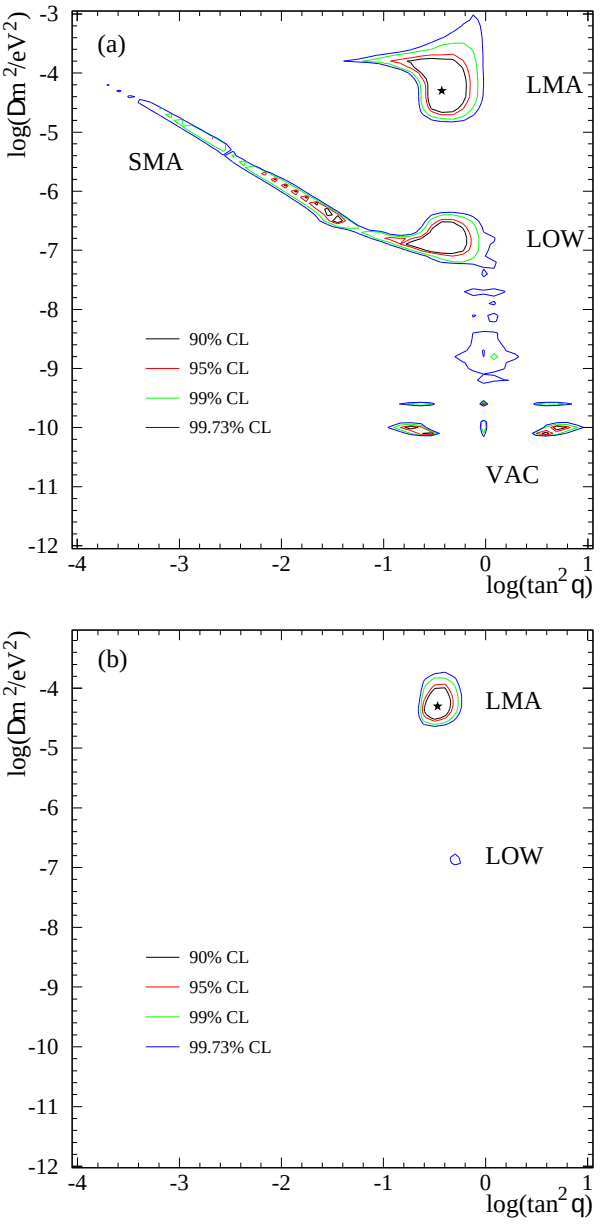

Figure 5: Allowed regions of the MSW plane determined by a χ^2 fit to (a) SNO day and night energy spectra and (b) with additional experimental and solar model data. The star indicates the best fit.